JOURNAL OF BACTERIOLOGY, Feb. 2006, p. 988–998 Vol. 188, No. 3
0021-9193/06/$08.00+0 doi:10.1128/JB.188.3.988–998.2006

Regulation of the Glucosyltransferase (*gtfBC*) Operon by CovR in *Streptococcus mutans*

Saswati Biswas and Indranil Biswas*

Basic Biomedical Sciences, School of Medicine, University of South Dakota, Vermillion, South Dakota 57069

Received 14 October 2005/Accepted 13 November 2005

Streptococcus mutans **is an important etiological agent of dental caries in humans. The extracellular polysaccharides synthesized by cell-associated glucosyltransferases (encoded by *gtfBC*) from sucrose have been recognized as one of the important virulence factors that promote cell aggregation and adherence to teeth, leading to dental plaque formation. In this study, we have characterized the effect of CovR, a global response regulator, on glucosyltransferase expression. Inactivation of *covR* in strain UA159 resulted in a marked increase in the GtfB and GtfC proteins, as analyzed by sodium dodecyl sulfate-polyacrylamide gel electrophoresis. With the use of a transcriptional reporter system of a single chromosomal copy of the P*gtfB-gusA* and P*gtfC-gusA* fusions, we confirmed the transcriptional regulation of these promoters by CovR. By in vitro electrophoretic mobility shift assays with purified CovR protein, we showed that CovR regulates these promoters directly. DNase I footprinting analyses suggest that CovR binds to large regions on these promoters near the transcription start sites. Taken together, our results indicate that CovR negatively regulates the expression of the *gtfB* and *gtfC* genes by directly binding to the promoter region.**

Streptococcus mutans is considered to be the principal etiological agent of dental caries (39). The abilities to metabolize carbohydrates and to adhere to and form tenacious biofilms on tooth surfaces are believed to be critically associated with the cariogenicity of this pathogen. In *S. mutans*, the extracellular polysaccharides synthesized from sucrose have been recognized as one of the important virulence factors for dental caries formation. *S. mutans* produces α-(1-3)- and α-(1-6)-linked glucan polymers synthesized by the cell-associated and secreted glucosyltransferases (GTFs) encoded by the *gtfB*, *gtfC*, and *gtfD* genes. The *gtfB* and *gtfC* genes are tandemly arranged and encode the GTF-I and GTF-SI enzymes, respectively, that synthesize water-insoluble, α-(1-3)-rich glucan. The GTF-S enzyme, encoded by *gtfD*, is responsible for water-soluble α-(1-6)-rich glucan synthesis. Water-insoluble glucans are a significant constituent of plaque biofilms that facilitate adherence and accumulation of stable biofilms mediated by glucan-binding proteins. Biofilm formation is influenced by the amount of GtfB and GtfC produced by *S. mutans* (43), and both GtfB and GtfC have been shown to be involved in adherence and cariogenesis in animal models (46, 60).

S. mutans also synthesizes four glucan-binding proteins: GbpA, GbpB, GbpC, and GbpD. The loss of any of the Gbps has an impact on adhesion or biofilm formation (3). For example, loss of GbpC (encoded by *gbpC*) changes the architecture of the sucrose-dependent biofilm deposited on experimental surfaces (2, 3). GbpC is a cell wall-associated protein and contains an LPXTG motif at the C terminus that is needed for sortase-mediated cell wall anchoring (50) and is actively involved in rapid, dextran-dependent aggregation during biofilm formation (50). It is assumed that GbpC is the cell surface glucan receptor originally predicted to explain dextran-dependent aggregation and sucrose-dependent cell association of GTFs and Gbps (3, 50).

Although GTFs and Gbps clearly contribute to dental plaque formation, the molecular mechanisms by which the genes that encode them are regulated are not clearly understood. The activity of GTF enzymes can be modulated by environmental conditions such as pH, ion concentration, and oxidation-reduction potential (reviewed in reference 45). Expression of *gtf* genes was originally thought to be constitutive, but recent analysis with reporter fusions (23, 37, 59) and direct measurements of specific mRNA (20) has identified several environmental signals, including pH, carbohydrate availability, and growth phase, which have profound effects on the expression of the *gftB*, *gtfC*, and *gtfD* genes. Since the *gtfB* and *gtfC* genes are very close together, it was originally thought that expression of the *gtfB* and *gtfC* genes was linked (56). However, recent data suggest that the expression of these two genes is not linked (21, 23, 53). Although we begin to understand how *gtfBC* genes are regulated, very little is known about the regulation of various Gbps.

Two-component signal transduction systems play important roles in bacterial gene expression in response to a variety of stimuli (16). These systems consist of a sensor kinase and an effector, or response regulator (RR), which is generally a DNA-binding protein that modulates the expression of certain target genes. In *S. mutans*, at least 13 complete two-component systems have been identified (1). Only a few two-component systems have been studied to a limited extent in this bacterium. In many cases, two-component regulatory systems are either implicated in or have been directly shown to regulate biofilm development (5, 38, 40, 52, 62). In *S. mutans*, at least three two-component systems were shown to be directly involved in biofilm formation (5, 32, 38).

The CovR/S two-component signal transduction system is a global regulator of virulence gene expression in group A and

* Corresponding author. Mailing address: Division of Basic Biomedical Sciences, University of South Dakota School of Medicine, Lee Medical Building, 414 East Clark Street, Vermillion, SD 57069. Phone: (605) 677-5163. Fax: (605) 677-6381. E-mail: ibiswas@usd.edu.

TABLE 1. Primers used in this study

Primer	Sequence (5′ to 3′)[a]	Purpose(s)
CovR R4	ACGCATGAAAACACCTCAGTTCTAAGACTC	CovR inactivation
Bam-CovR F4	ccgcggatccATTAATGAAGTTTTTGTCGAAAACA	CovR inactivation *covR* complementation (pIB30), P*cov-gusA* fusion, RNA blotting
Bam-CovR R2	gcgcggatccTTAATTATTTTCGCGAATGAATACCCCATGCC	*covR* complementation (pIB30), MBP-CovR expression (pIB7)
Eco-CovR F2	gcgcgaattcATGGCTAAGGACATTTTAATTATTGAAGATG	MBP-CovR expression (pIB7)
Xho-CovR-R5	cgcgctcgagATCGAAATCTTTTTCAAGTGCTC	P*cov-gusA* fusion, RNA blotting
CovR Fout 2	AACCTCATATCCTTCATGTTGTAATTCTAAAG	P*covR* primer extension
CovR Fout 4	GGGAAACTCCTTACGTTACTAAGG	P*covR* primer extension
Bam-GtfB F2	gcgcggatccACGTATTCGTGATAAGAAGAAACGT	P*gftB-gusA* fusion
Xho-GtfB R2	cgcgctcgagCCACCCGAAAGTGTAGTTAAAGTCA	P*gftB-gusA* fusion
Bam-GtfB F3	gcgcggatccAAGTAACTAACTCGTCGTTTCATTGC	GtfB EMSA, DNase I protection assay
Xho-GtfB R3	cgcgctcgagTTTGCGCAGTTTATAACGCACTTTC	GtfB EMSA, DNase I protection assay
GtfB Fout3	CACAGCAGATGCAACAGATACTGTCACCCATC	P*gtfB* primer extension
Bam-GtfC F1	gcgcggatccTAAGAGGGCGTTTCTAGGGTTAGGAG	GtfC EMSA, DNase I protection assay, P*gftC-gusA* fusion
Xho-GtfC R1	cgcgctcgagAGGTCAAAGTCACTACAGCTGAAGC	GtfC EMSA, DNase I protection assay, P*gftC-gusA* fusion
GtfC-Fout 1	GATACTGTCACCCATCTTTTCTTTACTTTACG	P*gtfC* primer extension
Smu-RpsL F	ATGCCTACAATTAACCAGTTGGTTCGTAAGCC	RpsL RNA blotting
Smu-RpsL R	GGTTTCTTAGTACCCATATTTAGAACGGCC	RpsL RNA blotting
Smu1405 R Sac	cgcggagctcCCAACCAGTATAATGACGTCTTTCCAGC	pIB105 construction
Smu1405 F	GTATGATAGTATCCTTTTATCAGGG	pIB105 construction

[a] Lowercase letters indicate restriction sites incorporated into primers.

group B streptococci (GAS and GBS, respectively). The RR CovR regulates about 15% of the genes in GAS; many of them are involved in pathogenesis (24). In GBS, CovR regulates at least 6% of the genes (36) and is essential for virulence (33). *S. mutans* also encodes a CovR ortholog, variously known as GcrR or TarC (32, 51); however, the CovS ortholog remains to be identified in *S. mutans* (1). It was previously shown that inactivation of *covR* in *S. mutans* led to altered biofilm formation, and the corresponding mutant was hypocariogenic (32, 51). Transcriptional analysis revealed that CovR represses at least two important genes, *gtfD* and *gbpC*, in *S. mutans* (32).

In this study, we have characterized the effect of CovR on *gtfB* and *gtfC* expression. Inactivation of *covR* in the UA159 strain resulted in a marked increase in the production of the GtfB and GtfC proteins as analyzed by sodium dodecyl sulfate (SDS)-polyacrylamide gel electrophoresis (PAGE). Reporter fusion analysis suggests that both these genes are regulated by CovR at the transcription level. In vitro DNA-binding assays with purified CovR protein showed that CovR binds directly to both the P*gtfB* and P*gtfC* promoters and protects from DNase I. This is the first step in understanding the mechanism of gene regulation by CovR, an important RR in *S. mutans*.

MATERIALS AND METHODS

Bacterial strains and growth conditions. *Escherichia coli* strain DH5α was grown in Luria-Bertani medium, and when necessary, ampicillin (100 μg ml^{-1}), kanamycin (100 μg ml^{-1}), and/or spectinomycin (100 μg ml^{-1}) were included. *S. mutans* UA159 is a standard laboratory strain that belongs to Bratthall serotype c. This strain was originally isolated by Page Caufield (University of Alabama, Birmingham), and its whole genome has been sequenced recently (1). *S. mutans* strains were routinely grown in Todd-Hewitt medium (BBL, Becton Dickinson) supplemented with 0.2% yeast extract (THY). When necessary, kanamycin (300 μg ml^{-1}), erythromycin (10 μg ml^{-1}), and/or spectinomycin (300 μg ml^{-1}) were included.

Construction of a *covR* deletion strain. The *covR* gene was insertionally inactivated in the UA159 strain by gene replacement. A 1.7-kb DNA fragment containing the entire *covR* gene and flanking regions was PCR amplified from UA159 genomic DNA with primers Bam-CovR F4 and CovR R4 (Table 1 contains the sequences of the primers used). The DNA fragment was cloned into the pGEMT-Easy TA cloning vector (Promega), and the resulting plasmid (pIB10) was confirmed by restriction analysis. A 1.4-kb spectinomycin resistance cassette (*aad9*) was isolated from plasmid pUCSpec (31) upon digestion with PstI and blunt ended. It was then ligated into a unique MfeI site (restricted and blunted with T4 polymerase) within the *covR* coding sequence, and the resulting construct was named pIB26. The orientation of the spectinomycin resistance cassette was verified by PCR. Since the *aad9* gene does not carry a terminator, it is expected that insertion of the *aad9* gene would be nonpolar. Plasmid pIB26 was linearized with NotI and then used to transform *S. mutans* strain UA159 according to a previously published protocol (11). Spectinomycin-resistant transformants were selected on THY agar containing the appropriate antibiotic, and PCR analysis with flanking primers and Southern hybridization with the entire region as a probe were done to confirm that *covR* inactivation had occurred by double-crossover recombination. This strain was named IBS10.

Construction of *covR*-complementing plasmid pIB30. To express the *covR* gene in *trans*, a PCR fragment containing the full-length *covR* gene and the 654 bp upstream of its start codon was amplified from UA159 by using primers Bam-CovR F4 and Bam-CovR R2, which introduced unique BamHI sites at both ends. The resulting 1.34-kb fragment was restricted with BamHI and cloned into BamHI-restricted plasmid pOri23 (49), an erythromycin resistance-encoding shuttle vector able to replicate in streptococci, to create pIB30. Plasmid pIB30 contains only the intact *covR* gene under its own promoter and no other downstream genes.

Construction of reporter strains. To construct a reporter strain, we chose the *Smu1405* locus into which to insert a reporter fusion. This locus encodes putative transposon-related proteins; therefore, we anticipate that inactivation of this locus will have no effect on gene regulation. A PCR fragment 1.1 kb in length corresponding to the *Smu1405* locus was amplified from UA159 with primers Smu1405-F and Smu1504-R-Sac. This PCR fragment was digested with KpnI and SacI and cloned into KpnI-SacI-digested pBluescript-SKII (Stratagene) to generate intermediate plasmid pIB105. In order to construct plasmids for reporter fusions, we isolated a *gusA* reporter gene. A 4.8-kb PacI-SacI fragment containing the *gusA* reporter gene and a kanamycin resistance gene was isolated from plasmid pJRS462 (8), blunt ended, and cloned into StyI (unique site in the middle of the *Smu1405* PCR fragment)-restricted pIB105. The resultant plasmid, pIB107, contains a gram-positive kanamycin resistance gene (*aphA3*) and a *gusA* gene flanked by Smu1405 fragments (upstream *Smu1405-aphA3-gusA*, downstream *Smu1405*). This pIB107 plasmid also contains unique BamHI and XhoI sites in front of the *gusA* gene. Promoters of interest can be cloned into the BamHI and XhoI sites of plasmid pIB107 for transcriptional reporter fusion. The

gftB promoter region (630 bp) was amplified from UA159 genomic DNA by using primers Bam-GtfB-F2 and Xho-GftB-R2 and cloned into BamHI-XhoI-restricted pIB107 to generate pIB113. Similarly, the *gtfC* promoter region (247 bp) was amplified from UA159 with primers Bam-GtfC-F1 and Xho-GftC-R1 and cloned into pIB107 to generate pIB118. Both pIB113 and pIB118 were linearized with BglI and transferred to UA159 by natural transformation to generate IBS137 and IBS138 by double crossover, respectively. Both the IBS137 and IBS138 reporter strains are kanamycin resistant due to presence of the *aphA3* gene in the reporter. Insertion of P*gtfBC-gusA* at the *Smu1405* locus was verified by PCR.

GusA assays. Specific activity of β-glucuronidase (GusA) was assayed essentially as previously described (8). Briefly, strains were grown to late exponential phase in THY broth and cell lysates were prepared for GusA activity. The GusA activity in the lysate was standardized by comparison to known concentrations of glucuronidase (Sigma). The protein concentration in the lysate was determined by the BCA protein assay (Pierce) standardized against bovine serum albumin.

Preparation of whole-cell extract and supernatant proteins. Overnight cultures were grown in THY, collected by centrifugation, and washed twice in one-half volume of phosphate-buffered saline. The cell density was adjusted to 5.0 cell units ml^{-1} (1 cell unit ml^{-1} is equivalent to 1 ml of culture at an optical density at 600 nm of 2.0), and total cell extracts were prepared by lysing the cell suspension with a glass bead beater as described for *S. pyogenes* (6). For culture supernatant proteins, cells were removed from fresh overnight culture by centrifugation, followed by filtration through a 0. 2-μm-pore-size filter. Proteins were obtained by precipitation with trichloroacetic acid (25% [wt/vol] final concentration) on ice for 2 to 4 h, washed with acetone, and resuspended in 1× gel loading buffer (NEB) to 1/40th volume.

Biofilm formation assay. Biofilms of *S. mutans* were grown in two different media. UA159 and its derivatives were grown overnight in THY medium at 37°C anaerobically. The culture was diluted 1:10 into fresh THY medium and incubated further for 6 h. The culture was then diluted 1:1,000 with either THY or BM (40) medium containing 1% sucrose. A 0.4- or 0.8-ml volume of this cell suspension was added to each well of an eight-well or four-well, respectively, glass chamber slide (Lab-Tek; Nalge Nunc International) for biofilm formation on glass. For biofilm formation on a polystyrene surface, U-bottom 96-well microtiter plates (Corning Inc.) were used. Biofilm was also formed on ceramic hydroxyapatite disks (0.5 in. in diameter by 0.05 in. thick; Clarkson Chromatography Products Inc.). The slides or microtiter plates were incubated at 37°C for 20 to 24 h as a static culture to allow biofilm formation. Biofilms were stained by 0.01% crystal violet and photographed. Biofilms formed on glass slides and on hydroxyapatite disks were analyzed by scanning electron microscopy (SEM). Slides and disks were washed once with sterile water, fixed with glutaraldehyde, and incubated at room temperature overnight. Following dehydration through a graded series of ethanol washes, slides were air dried, sputter coated with gold, and analyzed by SEM (ISI-60A; International Scientific Instruments) at various magnifications at the University of South Dakota core facility.

Primer extension analysis. UA159 was grown to mid-log or stationary phase as described above. Cells were collected by centrifugation, and total RNA was extracted with a FastRNA Blue kit (QBiogen) as described previously (8). Complementary oligonucleotides that were mapped to the 3′ side of the transcription start site (Table 1) were 5′ end labeled with [γ-^{32}P]ATP. Primer extension was carried out with SuperscriptII RNase H reverse transcriptase (Invitrogen) by following the manufacturer's recommended protocol. Samples were analyzed on a 6% denaturing sequencing gel with sequencing reaction mixtures (USB) as markers, followed by phosphorimaging.

Construction and purification of MBP-CovR. To generate a maltose binding protein (MBP)-CovR fusion protein, *covR* was amplified from the UA159 chromosome with primers Eco-CovR-F2 and Bam-CovR-R2. This PCR fragment was restricted with EcoRI and BamHI and cloned into EcoRI-BamHI-digested pMalC2 (New England Biolabs) to make pIB7. MBP-CovR from pIB7 was overexpressed in *E. coli* DH5α after cells were grown at 37°C to an optical density at 600 nm of 0.5. Expression was induced by addition of 1 mM isopropyl-β-D-thiogalactopyranoside (IPTG). Cells were grown for another 3 h at 37°C, collected by centrifugation, and resuspended in buffer A (20 mM Tris-Cl, pH 7.4, 200 mM NaCl, 2 mM 2-mercaptoethanol). Cells were lysed by sonication, and insoluble cell debris was removed by centrifugation. The cleared lysate was then passed over an amylase resin column (New England Biolabs) and washed with 6 volumes of buffer A. MBP-CovR was eluted from the column with 5 volumes of buffer A containing 10 mM maltose. Eluted MBP-CovR was dialyzed overnight in buffer containing 10% glycerol, 20 mM Tris-Cl, pH 7.4, 50 mM NaCl, 1 mM EDTA, 2 mM 2-mercaptoethanol, and 20 mM phenylmethylsulfonyl fluoride. The final concentration of MBP-CovR was measured by comparison with bovine serum albumin with the BCA kit, and aliquots of MBP-CovR were stored at −80°C.

Electrophoretic mobility shift assay (EMSA). PCR fragments were generated from the *gtfB* and *gtfC* promoters by using primers Bam-GtfB-F3 and Xho-GtfB-R3 and primers Bam-GtfC-F1 and Xho-GtfC-R1, respectively. PCR fragments were end labeled as described elsewhere (7). Various concentrations of MBP-CovR were incubated in DNA-binding buffer [50 mM $NaPO_4$, pH 6.5, 50 mM NaCl, 1 mM $MgCl_2$, 1 mM $CaCl_2$, 1 mM dithiothreitol, 2 μg/ml poly(dI-dC), 10% glycerol] in a final volume of 40 μl at room temperature for 40 min with 0.1 pmol of radiolabeled PCR fragments containing promoter elements of either *gtfB* or *gtfC*. If the protein was to be phosphorylated, 50 mM acetyl phosphate was added to the MBP-CovR in the DNA-binding buffer and incubated at room temperature for 45 min prior to the addition of radiolabeled PCR fragments. After incubation, samples were loaded onto a 50 mM $NaPO_4$-buffered (pH 6.5) 5% native acrylamide gel. Gels were run at room temperature at 120 V for approximately 3 h, dried, and exposed to a phosphorimager plate.

DNase I protection assay. MBP-CovR was allowed to bind to the same radiolabeled DNA fragments as described above, but after incubation at room temperature, 2 μl of a 0.02-U/ml solution of DNase I (Epicenter) was added and the mixture was incubated further at room temperature for 2 min. The DNA was precipitated, run on an 8% denaturing gel containing 7 M urea and 1× Tris-borate-EDTA buffer, and analyzed by autoradiography on a phosphorimager plate.

RESULTS

Construction and characterization of a *covR* mutant. To investigate the putative role of the orphan RR CovR in *S. mutans*, a *covR* mutant was constructed in strain UA159. The *covR* coding sequence was cloned and disrupted at amino acid position 70 by inserting a spectinomycin resistance gene before transferring it to the UA159 chromosome by allelic exchange. The double-crossover event was confirmed by PCR and Southern blot analysis (data not shown). The orientation of the spectinomycin resistance gene was determined by PCR and found to be the same as that of the *covR* gene (data not shown). In order to characterize the growth of the *covR* mutant strain (IBS10), its colony morphology and ability to form a biofilm on borosilicate glass and polystyrene microtiter plates were studied. The growth rates of both the wild-type and *covR* mutant strains in ThyB with and without 1% sucrose were the same (data not shown). However, we observed clumping in the *covR* mutants in THY containing 1% sucrose. Visible clumping was observed when the IBS10 culture reached mid-log phase (Fig. 1A). Interestingly, no differences in colony morphology between UA159 and IBS10 were found. Previously, a *covR* mutant of *S. mutans* strain UA130 was shown to form aberrant biofilms (32). Therefore, we tested IBS10 for the ability to form a biofilm on borosilicate glass and polystyrene surfaces. Cultures were grown in BM medium (40) with 1% sucrose or in THY with 1% sucrose for 48 h. As shown in Fig. 1B, biofilm formation was drastically reduced in IBS10 compared with its isogenic wild-type parent, UA159. When analyzed by SEM, the architecture of the biofilm formed by IBS10 appeared to be altered compared to that of UA159. The *covR* mutant formed large aggregates heterogeneously distributed throughout the biofilm matrix (Fig. 1C). Taken together, our results suggest that there are significant phenotypic differences between the *covR* mutant and wild-type UA159.

Altered protein expression in the *covR* mutant. Since the *covR* mutant produced altered biofilms, we wanted to compare the protein profiles of the wild type and the *covR* mutant mainly because the expression of two exported virulence factors, GbpC and GtfD, required for biofilm formation was re-

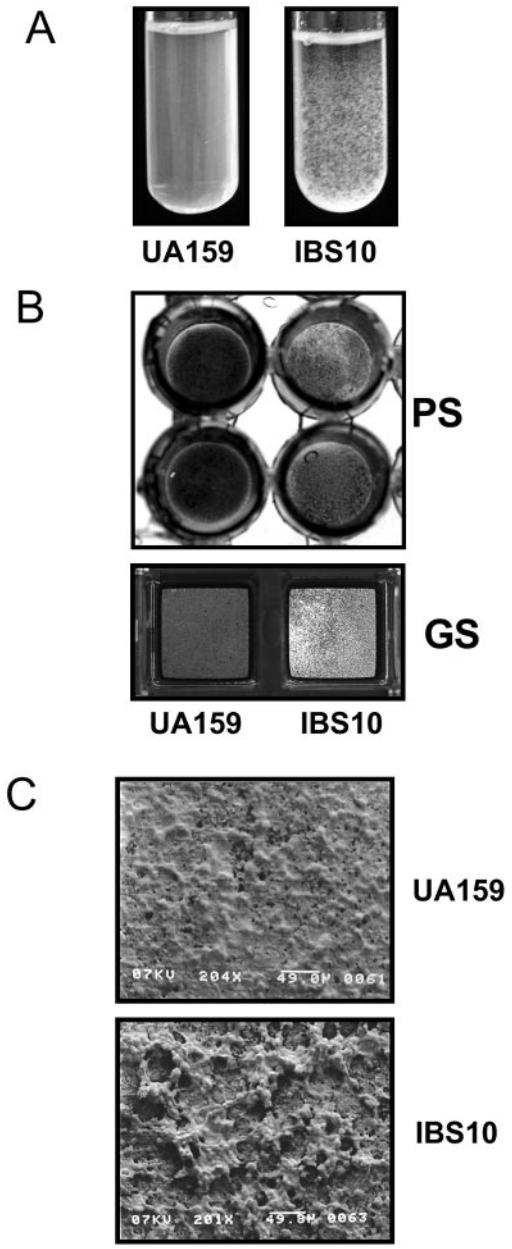

FIG. 1. Phenotypic characterization of *covR* mutants. (A) Log-phase cultures grown in THY plus 1% sucrose were photographed to demonstrate clumping. (B) Biofilm formation by UA159 and IBS10. Cultures were grown in BM medium with 1% sucrose at 37°C for 2 days. Cells attached to abiotic surfaces were stained with crystal violet. Upper part, biofilm on a polystyrene surface (PS; microtiter plate); lower part, biofilm on a glass surface (GS; eight-chambered glass slide). (C) Scanning electron micrographs of biofilms accumulated on hydroxyapatite disks.

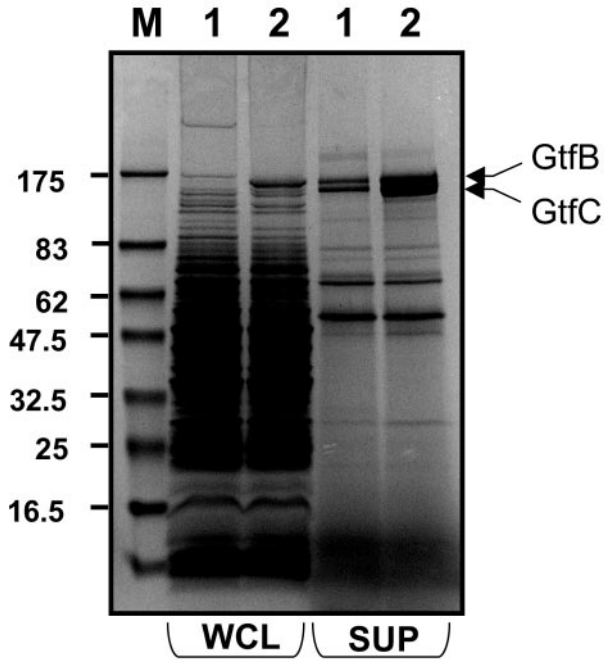

FIG. 2. Protein profiles of wild-type and *covR* mutant bacteria. Cells were grown to stationary phase in THY broth and separated from culture supernatant by centrifugation. Cells were lysed in phosphate-buffered saline to prepare whole-cell lysate. Culture supernatant proteins were precipitated with 25% trichloroacetic acid, washed, and resuspended in SDS-gel loading buffer. Samples were subjected to 4 to 20% SDS-PAGE and stained with Coomassie blue. Bands of interest were excised from the stained gel and subjected to mass spectrometric analysis. Lanes: M, NEB prestained marker; 1, whole-cell lysate (WCL) of UA159; 2, whole-cell lysate of IBS10; 3, culture supernatant (SUP) protein of UA159; 4, culture supernatant protein of IBS10. The values on the left are molecular sizes in kilodaltons.

cently shown to be affected by *covR* mutation in *S. mutans* (32, 51). The protein profiles of the wild type (UA159) and the *covR* mutant (IBS10) were determined for both total cellular and extracellular proteins by resolution via 4 to 20% gradient SDS-PAGE. As shown in Fig. 2, in the crude cell lysate of stationary-phase cells, two or three bands appeared to be over-expressed in the *covR* mutant. In the whole-cell lysate, several bands were up-regulated and several other bands were down-regulated in the mutant. Two distinct bands of approximately 170 kDa were elevated in the mutants compared to their wild-type counterpart. The larger band was overproduced in both the crude extract and the supernatant, while the lower band appeared to be overproduced only in the supernatant. But the lower band could be identified in comparable amounts in both the total cell extract and the culture supernatant fraction if the extracts were from the mid-log-phase cells (data not shown). To identify these two bands, we excised them from the gel and analyzed them by mass spectrometry. The larger protein was identified as GtfB, and the smaller protein was identified as GtfC. Thus, these results indicate that CovR either directly or indirectly represses the production of the GtfB and GtfC proteins in the cell and in the culture supernatant.

***covR* represses *gtfB* expression at the transcriptional level.** Since CovR is an RR (transcription factor) and since CovR was shown to repress the transcription of various genes in other streptococci, we asked whether CovR represses *gtfB* expression at the transcriptional level. To facilitate studies of gene regulation in *S. mutans*, a transcriptional reporter strain was constructed in a manner similar to that previously used for GAS (12) as described in Materials and Methods. The structure of the reporter construct is shown in Fig. 3A. Strain IBS137 contains a P*gtfB-gusA* transcriptional fusion in the

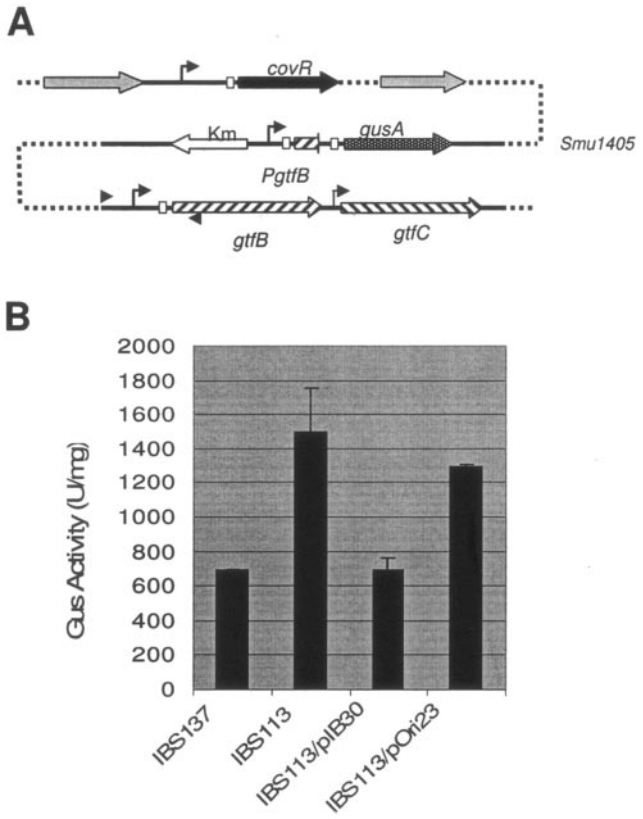

FIG. 3. Expression of the *gtfB* gene in the wild-type and *covR* mutant strains. (A). Gene organization in the P*gtf-gusA* reporter strain. The promoter region of *gtfB* with the sequence encoding the first 11 amino acids of GtfB was fused to the *gusA* reporter gene. The P*gtfB-gusA* reporter construct was inserted into the UA159 chromosome at the *Smu1405* locus (which is linked to neither the *covR* locus nor the *gtfBC* locus) to create IBS137. *covR* was inactivated in IBS137 to create IBS113. Symbols: bent arrow, promoters; white box, ribosome-binding site, dashed line, chromosomal region. Arrowheads indicate the primers used for P*gftB* promoter amplification. (B). GusA activity in the wild-type and *covR* mutant strains. Samples were collected at mid-exponential phase for determination of glucuronidase activity. The values shown are units of glucuronidase activity (with standard errors of the mean of experiments repeated at least twice).

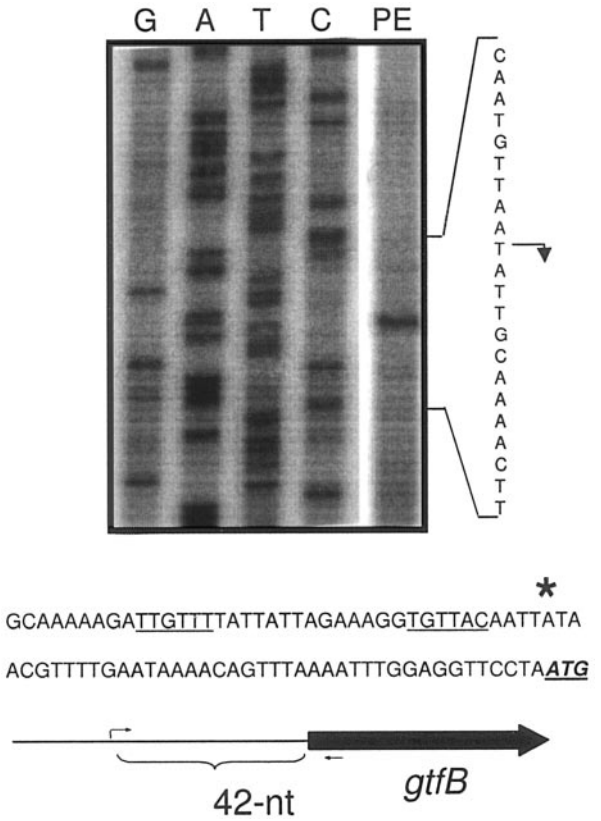

FIG. 4. Primer extension analysis at the *gtfB* promoter region. RNA was isolated from strain UA159 and used for primer extension analysis. The DNA sequences generated from the *gtfB* gene with the same primer (G, A, T, and C) are shown on the left, and the primer extension product is indicated by bent arrows. The DNA sequence (antisense strand) is shown. The putative transcriptional start site is shown by an asterisk, and the −35 and −10 regions are underlined. The italicized sequence is the beginning of the *gtfB* open reading frame. nt, nucleotides.

chromosome, and both the native *covR* and *gtfBC* loci are unaltered in this strain. To study the effect of CovR on *gtfB* expression, *covR* was inactivated in the IBS137 strain with plasmid pIB26 to generate IBS113. Transcription of P*gtfB* was quantitated in these strains by measuring the activity of GusA produced from the P*gtfB-gusA* reporter fusion (Fig. 3B). For this assay, cells were grown in THY broth and harvested in the late exponential phase. We found that *covR* mutant strain IBS113 showed twofold more P*gtfB-gusA* expression than *covR*$^+$ parent strain IBS137. To be sure that this effect was caused by the *covR* mutation, complementation experiments were done. A DNA fragment including *covR* with its potential promoter region was cloned into pOri23, which replicates in *S. mutans*, to generate pIB30. This plasmid contains only the *covR* gene and no other downstream genes. As a control, we used IBS113 containing the vector pOri23. This control strain had essentially the same GusA activity as strain IBS113 (86% activity), while the complemented strain, IBS113/pIB30, expressed about the same as the parental IBS137 strain. Thus, when *covR* was expressed in *trans* from a multicopy plasmid, P*gtfB* expression was decreased to the wild-type level. Therefore, it appears that CovR represses expression from the P*gtfB* promoter. Since we could complement the phenotype with just *covR* alone, this rules out the possibility that other downstream genes are involved in the process.

Mapping of the transcription start site of the *gtfB* gene. In order to analyze the regulation of *gtfB* expression by CovR, it was necessary to map precisely the start site within the upstream intergenic region of *gtfB*. We performed primer extension analysis with RNA extracted from UA159. Extension of the RNA with a *gtfB*-specific primer gave rise to a single band that mapped at 42 nucleotides upstream of the ATG start codon (Fig. 4). Analysis of the sequence upstream of the mapped 5′ RNA ends reveals a poorly conserved −10 sequence (TgTtAc, uppercase denotes consensus) and a poorly conserved −35 region (TTGttt). Since the −10 sequence is very poorly conserved, it is possible that the observed site may be due to RNA processing. Sequence analysis of the immediate upstream region of P*gtfB* (275 bp) failed to identify any other promoter-like sequences. Moreover, a fragment carrying this region showed

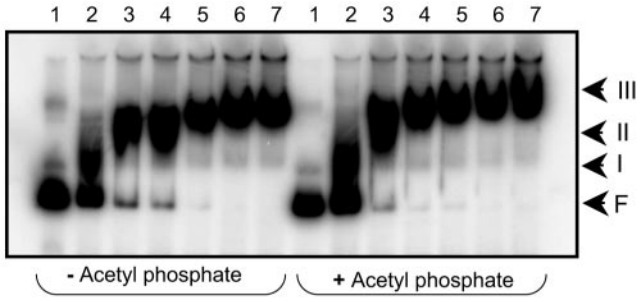

FIG. 5. CovR binding to a DNA fragment containing P*gtfB*. EMSA with CovR (left) and CovR preincubated (45 min) with 50 mM acetyl phosphate (right). The concentrations of protein added to 0.1 pmol of the 351-bp P*gtfB* sequence are as follows: lane 1, 0 μM; lane 2, 1 μM; lane 3, 2 μM; lane 4, 4 μM; lane 5, 6 μM; lane 6, 8 μM; lane 7, 10 μM. The arrows on the right indicate the forms of the CovR-P*gtfB* DNA complex. F, free DNA.

promoter activity (see below), indicating that the observed primer extension product may be the authentic transcription start site. Thus, the transcription start site of the *gtfB* gene is very close to the translation start site.

CovR binds the promoter sequence of the *gtfB* gene. As shown above, expression of *gtfB* is repressed by the CovR RR. In order to determine whether this repression is direct, we studied the binding of CovR to the *gtfB* promoter region. We cloned the *covR* coding sequence into an expression vector that allowed overexpression of an amino-terminal MBP-CovR fusion protein. This construct was selected because similar amino-terminal fusion constructs from the GAS CovR ortholog were found to bind indistinguishably from native CovR (19). The MBP-CovR fusion protein from *S. mutans* remained soluble when overexpressed in *E. coli* and was purified over an amylase column. This fusion protein was >95% pure, as revealed by Coomassie staining (data not shown).

To study binding of purified MBP-CovR protein, a 351-bp PCR fragment that included positions −275 to +76 (with respect to the start of transcription) of P*gtfB* was used in a gel mobility shift assay. As shown in Fig. 5, we found that purified MBP-CovR bound a DNA fragment containing P*gtfB*. In the binding assays, three retarded forms were observed (Fig. 5, arrows). At a CovR concentration of 1 μM, the predominant CovR-P*gtfB* complex is form I, and at concentrations of 2 to 8 μM, slower-migrating complexes (forms II and III) are visible. To show the specificity of binding, we performed competition assays. Addition of a 50-fold molar excess of a similarly sized, unlabeled DNA fragment containing *rpsL*, a constitutively expressed gene, had no effect on binding, whereas addition of a 25-fold molar excess of the unlabeled P*gtfB* fragment eliminated binding to the labeled P*gtfB* fragment (data not shown).

Because the affinity for DNA of two-components regulators often depends on their phosphorylation state and because it has been shown previously that addition of phosphate to MBP-CovR of GAS increases its affinity for target DNA (4, 19, 44), we asked whether addition of phosphate would increase the affinity of purified MBP-CovR for P*gtfB* DNA. Prior incubation of MBP-CovR with acetyl phosphate, a small-molecule phospho donor routinely used for phosphorylation, did not increase its affinity for P*gtfB*. Therefore, phosphorylation apparently has no effect on CovR binding. Because we did not determine the efficiency of phosphorylation of CovR by acetyl phosphate, we cannot rule out the possibility that addition of acetyl phosphate did not change the phosphorylation status of CovR.

CovR binds to a large region near the *gftB* promoter. To identify the region within P*gtfB* important for CovR binding, we used a DNase I protection assay. The P*gtfB* probe used for this is the same 351-bp PCR fragment used in the gel mobility shift assay, except that the DNA was end labeled only on one strand. As shown in Fig. 6, MBP-CovR binding resulted in a large DNase I footprint on P*gtfB* that surrounded the −35 and −10 sequences, whose size and/or intensity increased with increasing protein concentrations (Fig. 6, lanes 2 to 5). Based on the sequencing ladder that was run alongside, we found that the total protected region was approximately 150 bp and spanned positions −110 to +33 (+1 is the transcription start site) of P*gtfB*. Therefore, CovR protects a large region of the P*gtfB* promoter covering the −35 and −10 sequences.

CovR also regulates P*gtfC* expression. Because we observed increased GtfC expression in the *covR* mutant and because *gtfC* has its own promoter (in addition to expression from the *gtfB* promoter), we asked whether CovR also regulates this P*gtfC* promoter independently of P*gtfB*. We first tested expression of P*gtfC* by generating a P*gtfC-gusA* reporter fusion as described in Materials and Methods. Strain IBS138 contains a P*gtfC-gusA* transcriptional fusion in the chromosome. As before, *covR* was inactivated in IBS138 by allelic exchange to create IBS114. Transcription of P*gtfC* was quantitated in these strains by measuring the GusA activity produced from the P*gtfC-gusA* reporter fusion (Fig. 7A). We found that overall transcription from P*gtfC* was approximately three- to fourfold lower compared to that from P*gtfB* in the wild-type background. We also found that inactivation of *covR* increased P*gtfC* expression. The difference was 1.5-fold (statistically significant). In order to confirm that increased P*gtfC* expression was indeed caused by *covR* mutation, IBS114 was complemented with pIB30. As expected, IBS114/pIB30-produced P*gtfC* expression was similar to that produced by wild-type IBS138, while the vector control strain IBS114/pOri23 did not change P*gtfC* expression. Thus, like P*gtfB*, P*gtfC* is repressed by CovR at the transcriptional level.

In order to map the exact transcription start site within the upstream intergenic region of P*gtfC*, we performed primer extension with RNA extracted from UA159. We obtained two products that were mapped at 43 and 45 nucleotides upstream from the ATG start codon of *gtfC*. A fairly conserved −10 sequence (TAcAAT) and −35 sequence (TTGtgc) were found upstream of the 5′end of the RNA. Taken together, these findings suggest that *gtfC* is expressed from its own promoter, as reported previously (21, 23, 53), and is regulated by CovR.

To determine whether this regulation is direct, we studied the binding of CovR to the P*gtfC* promoter. We made a PCR product of 247 bp corresponding to positions +125 to −132 (with respect to the transcription start site) and used it in a DNA-binding assay. As shown in Fig. 7C, MBP-CovR increasingly bound to the P*gtfC* promoter DNA fragment with increasing amounts of protein. We also observed three retarded species in the gel shift assay, similar to what we observed with the P*gtfB* promoter. Addition of a 50-fold molar excess of the unlabeled *rpsL* fragment, had no effect on binding (data not

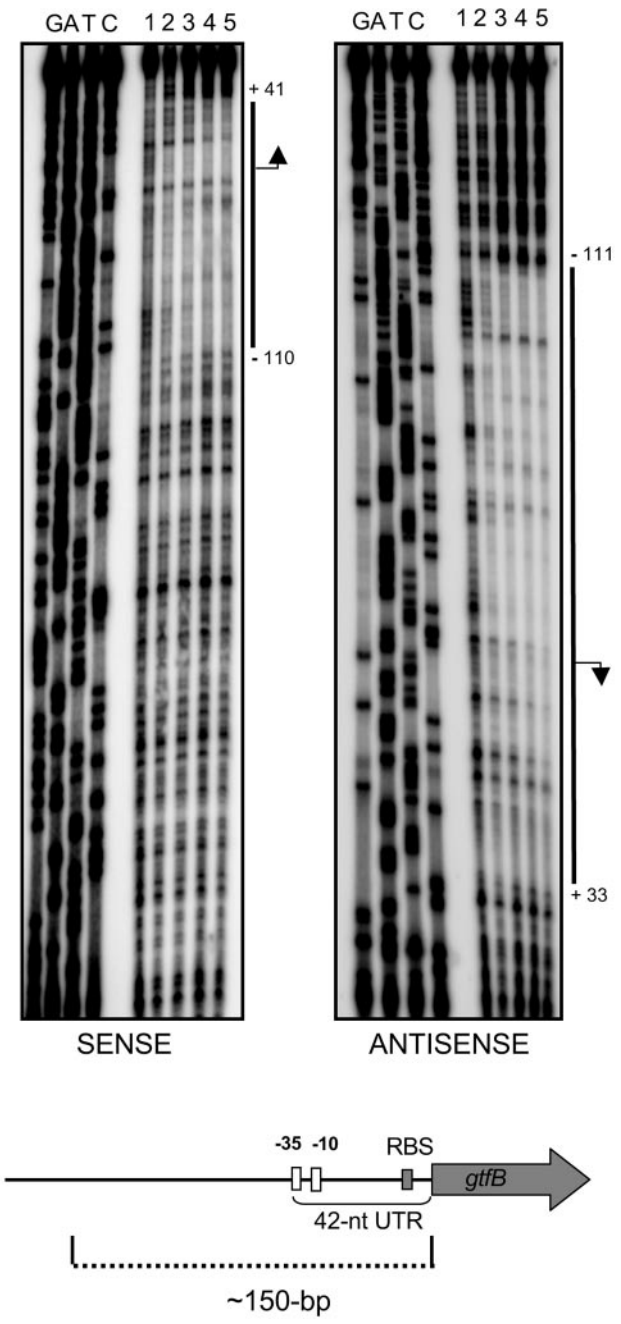

FIG. 6. DNase I protection assay of the P*gtfB* promoter. An EMSA was done with MBP-CovR and a 351-bp P*gtfB* DNA sequence as described in the legend to Fig. 5. The concentrations of protein added to 0.1 pmol of the 351-bp P*gftB* DNA sequence were 0, 2, 4, 8, and 10 μM (lanes 1 to 5, respectively). A DNase I protection assay was done as described in the text. Footprints were run in an 8% sequencing gel next to sequencing ladders (G, A, T, and C). A schematic diagram showing the protected region at the P*gtfB* promoter is at the bottom. It appears that CovR protects about 150 bp at the P*gtfB* promoter. The bent arrow shows the start of transcription. RBS, ribosome-binding site; nt, nucleotides; UTR, untranslated region.

shown). Taken together, our results suggest that CovR specifically binds to multiple sites of P*gtfC*.

DNase I footprinting assays were then performed to localize those DNA-binding sites of CovR on the P*gtfC* promoter. We used the same 257-bp fragment that was used in the gel shift assay. We found that the DNase I protection region on P*gtfC* is comparatively smaller than that on P*gtfB* and spans positions +101 to +5 (Fig. 7D). Therefore, our results show that CovR also regulates P*gtfC* expression by binding directly to the promoter.

DISCUSSION

The CovR proteins are very important RRs that influence virulence gene expression in streptococci. In the case of *S. mutans*, CovR has been shown to repress the *gbpC* gene, encoding a glucan-binding protein, and the *gtfD* gene, encoding a GTF that produces water-soluble glucans (32, 51). These enzymes are involved in sucrose-dependent adherence and cariogenesis. A *covR* knockout strain was subsequently shown to form an altered biofilm and was hypocariogenic (32). In this study, we characterized a *covR* mutant of strain UA159. As previously noted (32, 50), we also found that the *covR* mutant formed cellular aggregates in liquid culture and showed altered biofilm formation. Notably, we also found that inactivation of *covR* caused increased production of Gtf-I and Gtf-SI, which are encoded by *gtfB* and *gtfC*, respectively. These GTFs are surface-associated extracellular proteins that facilitate adherence and colonization. GtfB and GtfC catalyze the cleavage of sucrose to synthesize water-insoluble glucans, which function as adhesins that help bacteria to anchor to the tooth pellicle (26, 47).

Although the role of GtfB and GtfC in *S. mutans* virulence is well established, the mechanisms that control the expression of these proteins are poorly understood. The *gtfB* and *gtfC* genes are tandemly arranged, and there is a 198-bp intergenic region between them. There is also a 448-bp intergenic region upstream of the *gtfB* gene. Although it is thought that these genes are cotranscribed (55), recent studies showed that *gtfB* and *gtfC* are independently expressed (21, 23, 53). A number of studies indicate that expression of theses genes is dependent on nutritional and environmental conditions, including growth rate, pH, carbon source, and whether the bacteria are grown under biofilm conditions (10, 29, 37, 59). The expression of *gtfB* seems to be higher than that of *gtfC*. By using a real-time PCR assay, Fujiwara et al. showed that the mRNA level of *gtfB* is approximately 16-, 15-, and 69-fold more than the level of *gtfC* mRNA during the early, middle, and late exponential phases of growth, respectively (20). When we measured Gus activity, we found that P*gtfB-gusA* expression is three- to fourfold higher than P*gtfC-gusA* expression (Fig. 3 and 7B). This is consistent with previous studies (20) and correlates with the optimal ratio that induces sucrose-dependent biofilm formation (48). However, a plasmid-based reporter system revealed that the expression of *gtfC* is approximately 10 times higher than that of *gtfB* (23). This difference in observations could be attributed to the variation of plasmid copy number between the two reporter strains. Alternatively, upstream regions present in the plasmid-based reporter system may not be sufficient to demonstrate the complete regulation pattern.

Several specific factors are also known to affect the expression of *gtfBC*. For example, the interspecies signaling system mediated by the *luxS* gene regulates *gtfBC* expression (61), although the specific mechanism by which the LuxS system affects *gtfBC* expression is not known. Another transcription

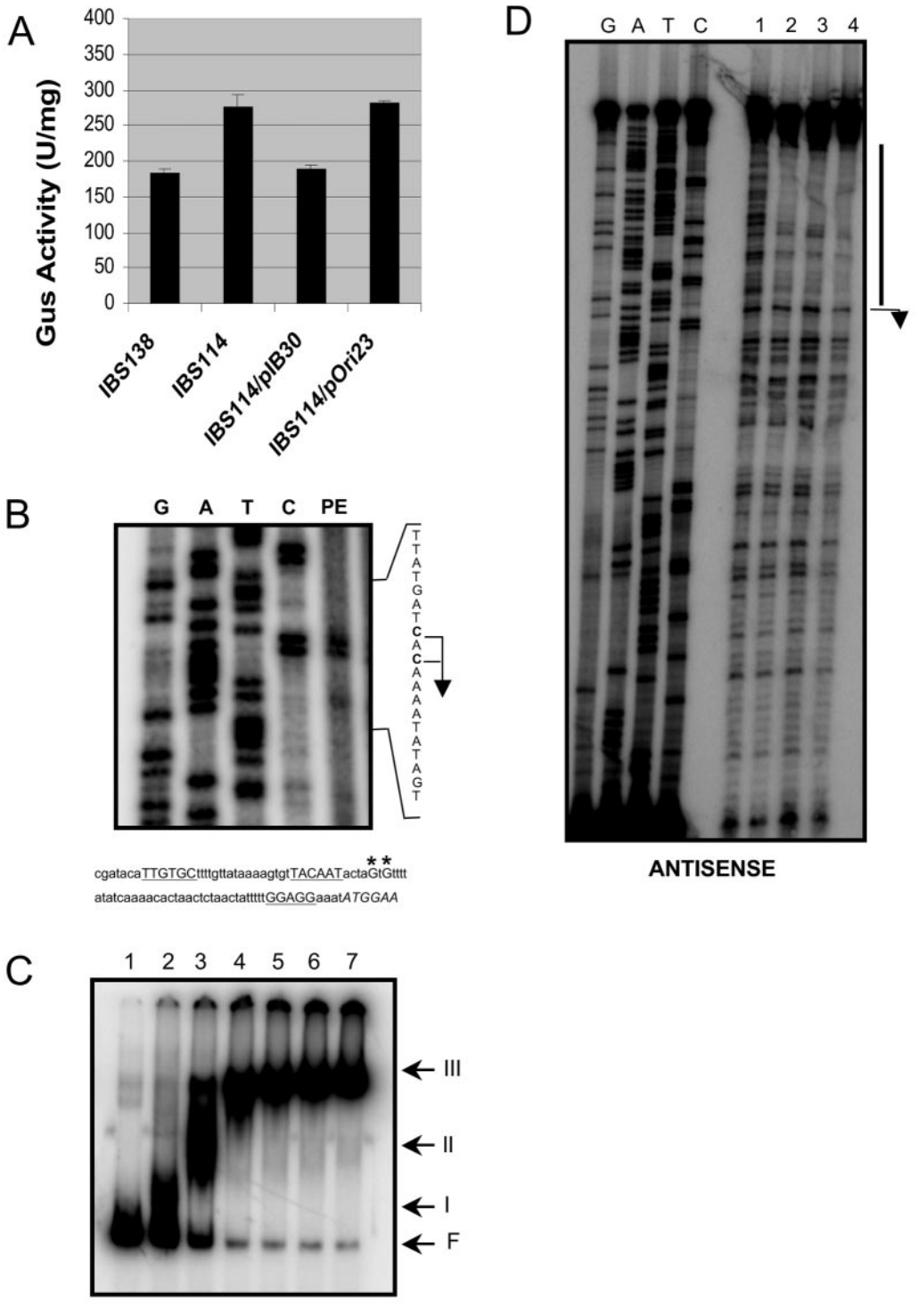

FIG. 7. Analysis of *gtfC* promoter expression. (A) Expression of P*gtfC* in the wild-type and *covR*-inactivated strains. The promoter region of *gtfC* (257 bp), along with the sequence encoding the first 29 amino acids of GtfC, was fused to the *gusA* reporter gene to generate the IBS138 and IBS114 strains. In strain IBS114, *covR* was also inactivated. Gus activity was measured as described in the legend to Fig. 2. The values shown are units of Gus activity per milligram of protein, with standard errors of the mean of experiments repeated twice. Both differences are statistically significant. (B) Mapping of the P*gtfC* promoter. RNA was extracted from strain UA159 and used for primer extension analysis. The DNA sequences were generated from P*gtfC* with the same primer (G, A, T, and C). The primer extension product is indicated by bent arrows. The DNA sequence (antisense strand) is shown. The putative transcriptional start sites are shown by asterisks, and the −35 and −10 regions are underlined. The italicized sequence is the beginning of the *gtfC* open reading frame. (C). Binding of CovR to the P*gtfC* promoter. An EMSA was done with a DNA fragment (257 bp) derived from the P*gtfC* region. The amounts of MBP-CovR are the same as in Fig. 5. The arrows on the right designate the forms of CovR-P*gtfC* DNA complexes. (D). DNase I protection assay of P*gtfC*. DNase I footprinting was done with the same DNA fragment as in the EMSA but labeled on the antisense strand. The concentrations of protein added to 0.1 pmol of DNA were 0, 2, 4, and 8 μM (lanes 1 to 4, respectively). The bent arrow denotes the transcription start site.

factor, RegM, a protein similar to catabolite control protein A (CcpA), also activates *gtfBC* expression as much as 10-fold, depending on the pH and glucose content of the medium (9). In gram-positive bacteria, CcpA-mediated gene regulation can occur via two different mechanisms (58). CcpA can regulate gene expression by binding directly to the promoter region of the regulated gene at the *cis*-acting replication element (CRE) sequence (42) or by altering the phosphorylation state of the HPr protein, a key component of the sugar:phosphor transfer system (41). The consensus sequence for the CRE has been deduced to be TGWNANCGNTNWCA (30). Analysis of the upstream intergenic regions suggests that several degenerate CRE sequences are present at or near the transcription start sites of both the *gtfB* and *gtfC* genes (9, 23). However, whether RegM binds to these sequences and their role in gene expression have yet to be determined. Recently, a two-component system, VicRK, was shown to activate *gtfBC* expression (52). The VicRK system is best characterized in *S. pneumoniae* and *Bacillus subtilis* (17, 28, 57). This system is essential for cell viability in all the bacteria so far studied (17, 18, 52, 57). The RR VicR directly binds to both the *gtfB* and *gtfC* promoters and presumably activates gene expression. A consensus VicR-binding sequence (TGTWAHNNNNNTGTWAH) that seems to serve across many gram-positive organisms was determined by Dubrac and Msadek (14). As described by Senadheera et al. (52), two partially conserved VicR-binding sites are present upstream of *gtfB* (−126 to −110 and −147 to −138) and one perfectly conserved consensus is present upstream of *gtfC* (−26 to −10). However, there is no experimental evidence that VicR binds to these sequences.

Our results suggest that CovR also regulates both *gtfB* expression and *gtfC* expression and that this regulation is direct since CovR binds to both the *gftB* and *gtfC* promoters. It appears that multiple binding sites are present on both the *gftB* and *gtfC* promoters since we saw at least three retarded species in the gel mobility shift assay. These multiple retarded species are also seen in the case of GAS CovR binding to the *hasA* promoters and other CovR-regulated promoters (19, 44). We also observed a large (~100-bp) footprint in a DNase I protection assay on both of the promoters. The protected region was centered on the transcriptional start sites, indicating that binding of CovR to these regions would be expected to inhibit transcription. The large footprint is a common feature of CovR binding to target genes that are generally repressed. For example, Miller and colleagues (44) showed that the average footprint for various target promoters for GAS CovR binding is about 110 bp. Since CovR binds to multiple sites in a given target promoter, it is expected to have a large footprint (19, 25). We speculate that CovR binding also leads to structural changes such as bending or looping at the target promoters.

In the case of GAS CovR, two different consensus binding sequences have been proposed. Miller et al. (44) proposed a 16-bp motif, T(T/A)ATTTTTAA(A/T)AAAA(C/A), which is present in the majority of promoters regulated by CovR. However, based on detailed analysis of multiple binding sites present on a single promoter (*hasA* promoter), Federle and Scott (19) proposed a smaller hexanucleotide motif, ATTARA. This motif is present in all of the binding sites on the P*hasA* promoter, and mutations in this motif interfered with CovR binding and CovR-mediated repression. While this motif is important for DNA binding, CovR can also bind to promoter regions that are devoid of this ATTARA sequence (25). For GBS CovR, a nonanucleotide motif (TATTTTAAT) has been proposed for the consensus sequence. While this sequence is clearly different from those reported to be recognized by GAS CovR, the only similarity is that all are AT rich. Although these sequences may play an important role in DNA binding, they may not be sufficient for recognition of the target promoter by CovR, since they occur more frequently in the genome than do the genes regulated by CovR (24, 36).

When we analyzed the DNase I-protected regions, we did not find any 16-bp GAS consensus motif (44) in the P*gtfB* or P*gtfC* promoter. But we found one ATTARA sequence (19) only on the P*gtfB* promoter. We also did not find any GBS CovR consensus (36) DNA-binding site on either of these two promoters. This indicates that *S. mutans* CovR recognizes a motif different from that of the GAS or GBS consensus sequence. Our results only suggest that CovR binds to large regions on the target promoters but do not give any indication of the minimal binding site necessary for CovR. Sequence comparison of the DNase I-protected regions from *gtfB* and *gftC* revealed that the most common feature between these two promoters is the high degree of AT-rich 6- to 8-bp motifs. In addition, we found a unique decanucleotide motif, GTGTTA CAAT, present in the protected regions of both P*gtfB* and P*gtfC*. We do not know the significance of this decanucleotide motif or other small AT-rich motifs in CovR binding. Experiments are under way to determine their role in DNA binding.

For many RRs, phosphorylation changes the conformation of the protein in such a way that either its affinity for the target DNA is enhanced or the oligomerization state is altered (27, 35). In the case of GAS CovR, phosphorylation leads to at least a twofold increase in its affinity for its target promoters and extends the region of DNase I protection (19, 25). Moreover, GAS CovR has also been shown to form oligomers upon phosphorylation (44). On the contrary, we did not find any obvious difference in affinity for the P*gtfB* (Fig. 5) or P*gtfC* (data not shown) promoter sequence when CovR was preincubated with acetyl phosphate. The fact that phosphorylation of CovR had no detectable effect on DNA binding is not surprising. The effect of phosphorylation of some RRs can be very specific, depending on the promoter structure (54). Thus, it is possible that the phosphorylation status of CovR does not alter its effect on P*gtfB*. Alternatively, since in this organism CovR appears to be an orphan (no cognate CovS), it is possible that phosphorylation does not play any role in CovR-mediated gene expression. However, like *S. mutans* CovR, CovR from GBS also binds to its target promoter with equal affinity with or without acetyl phosphate treatment (36). This difference in behavior among the *S. mutans*, GAS, and GBS CovR proteins could be attributed to their sequence difference, which is as much as 75%.

Like many other RRs, CovR also binds to multiple sites on the P*gtfB* and P*gtfC* promoters. In most cases, an RR bound at one site influences binding to nearby sites. Although it was not measured directly, however, our DNA-binding results suggest that CovR binding to the promoters tested does not appear to be cooperative, because increasing amounts of CovR resulted in the formation of multiple retarded complexes. This is not surprising since the mode of CovR binding varies significantly,

depending on the promoter. For example, GAS CovR binds to the P*has* and P*cov* promoters noncooperatively (19, 25) but binding to the P*sag* promoter is highly cooperative (22). In this case, phosphorylation also played a significant role in cooperative DNA binding (22).

CovR is an important global regulator which is directly involved in the pathogenesis of GAS and GBS (15, 33). In these organisms, CovR acts as both an activator and a repressor for a large number of genes (24, 36). In the case of *S. mutans*, CovR has been shown to be required for cariogenesis (32). So far, only four genes have been shown to be regulated by CovR; however, they all are important virulence factors necessary for biofilm development and pathogenesis. Although all the genes so far described are repressed by CovR, we have seen that CovR can also activate some other virulence factors (I. Biswas, unpublished data). Although CovR-controlled genes belong to the surface-associated or secreted proteins in GAS, GBS, and *S. mutans*, CovR is also involved in bacterial stress responses. In GAS, Dalton and Scott (13) showed that the CovR/S system responds to several stress conditions. Under stress conditions, CovS inactivates CovR, either directly or indirectly, to derepresses GAS genes needed for growth under stress and genes involved in virulence. Like GAS, CovR in *S. mutans* is also inactivated by several stress conditions (51), although the mechanism for this is not known and no CovS ortholog has been identified in *S. mutans*. Efforts are currently being made to identify the environmental cues to which CovR responds and to identify the cognate sensor kinase for CovR.

In conclusion, this work provides significant insight into important regulatory functions of CovR in *S. mutans*. However, further studies are necessary to define the complete CovR regulon, which are currently being pursued in our laboratory. Determining the nature of the interaction between CovR and its target promoters is the first step toward understanding the CovR signaling pathway. Deciphering the molecular mechanism(s) and identifying genes directly regulated by CovR can improve our understanding of virulence gene regulation in *S. mutans* and facilitate the identification of novel targets suitable for drug development to control cariogenesis.

ACKNOWLEDGMENTS

We thank Keith Weaver for critically reading the manuscript. We thank Said Suleman for technical help with the SEM analysis and Eduardo Callegari for mass spectrometric analysis.

This publication was made possible in part by an NIH grant (2 P20 RR016479) from the INBRE program of the NCRR and by a South Dakota Governor's 2010 Initiative grant.

REFERENCES

1. **Ajdic, D., W. M. McShan, R. E. McLaughlin, G. Savic, J. Chang, M. B. Carson, C. Primeaux, R. Tian, S. Kenton, H. Jia, S. Lin, Y. Qian, S. Li, H. Zhu, F. Najar, H. Lai, J. White, B. A. Roe, and J. J. Ferretti.** 2002. Genome sequence of *Streptococcus mutans* UA159, a cariogenic dental pathogen. Proc. Natl. Acad. Sci. USA **99:**14434–14439.
2. **Banas, J. A., K. R. Hazlett, and J. E. Mazurkiewicz.** 2001. An in vitro model for studying the contributions of the *Streptococcus mutans* glucan-binding protein A to biofilm structure. Methods Enzymol. **337:**425–433.
3. **Banas, J. A., and M. M. Vickerman.** 2003. Glucan-binding proteins of the oral streptococci. Crit. Rev. Oral Biol. Med. **14:**89–99.
4. **Bernish, B., and I. van de Rijn.** 1999. Characterization of a two-component system in *Streptococcus pyogenes* which is involved in regulation of hyaluronic acid production. J. Biol. Chem. **274:**4786–4793.
5. **Bhagwat, S. P., J. Nary, and R. A. Burne.** 2001. Effects of mutating putative two-component systems on biofilm formation by *Streptococcus mutans* UA159. FEMS Microbiol. Lett. **205:**225–230.
6. **Biswas, I., P. Germon, K. McDade, and J. R. Scott.** 2001. Generation and surface localization of intact M protein in *Streptococcus pyogenes* are dependent on *sagA*. Infect. Immun. **69:**7029–7038.
7. **Biswas, I., and P. Hsieh.** 1997. Interaction of MutS protein with the major and minor grooves of a heteroduplex DNA. J. Biol. Chem. **272:**13355–13364.
8. **Biswas, I., and J. R. Scott.** 2003. Identification of *rocA*, a positive regulator of *covR* expression in the group A streptococcus. J. Bacteriol. **185:**3081–3090.
9. **Browngardt, C. M., Z. T. Wen, and R. A. Burne.** 2004. RegM is required for optimal fructosyltransferase and glucosyltransferase gene expression in *Streptococcus mutans*. FEMS Microbiol. Lett. **240:**75–79.
10. **Burne, R. A., Y. Y. Chen, and J. E. Penders.** 1997. Analysis of gene expression in *Streptococcus mutans* in biofilms in vitro. Adv. Dent. Res. **11:**100–109.
11. **Burne, R. A., Z. T. Wen, Y. Y. Chen, and J. E. Penders.** 1999. Regulation of expression of the fructan hydrolase gene of *Streptococcus mutans* GS-5 by induction and carbon catabolite repression. J. Bacteriol. **181:**2863–2871.
12. **Caparon, M. G., and J. R. Scott.** 1991. Genetic manipulation of pathogenic streptococci. Methods Enzymol. **204:**556–586.
13. **Dalton, T. L., and J. R. Scott.** 2004. CovS inactivates CovR and is required for growth under conditions of general stress in *Streptococcus pyogenes*. J. Bacteriol. **186:**3928–3937.
14. **Dubrac, S., and T. Msadek.** 2004. Identification of genes controlled by the essential YycG/YycF two-component system of *Staphylococcus aureus*. J. Bacteriol. **186:**1175–1181.
15. **Engleberg, N. C., A. Heath, A. Miller, C. Rivera, and V. J. DiRita.** 2001. Spontaneous mutations in the CsrRS two-component regulatory system of *Streptococcus pyogenes* result in enhanced virulence in a murine model of skin and soft tissue infection. J. Infect. Dis. **183:**1043–1054.
16. **Fabret, C., V. A. Feher, and J. A. Hoch.** 1999. Two-component signal transduction in *Bacillus subtilis*: how one organism sees its world. J. Bacteriol. **181:**1975–1983.
17. **Fabret, C., and J. A. Hoch.** 1998. A two-component signal transduction system essential for growth of *Bacillus subtilis*: implications for anti-infective therapy. J. Bacteriol. **180:**6375–6383.
18. **Federle, M. J., K. S. McIver, and J. R. Scott.** 1999. A response regulator that represses transcription of several virulence operons in the group A streptococcus. J. Bacteriol. **181:**3649–3657.
19. **Federle, M. J., and J. R. Scott.** 2002. Identification of binding sites for the group A streptococcal global regulator CovR. Mol. Microbiol. **43:**1161–1172.
20. **Fujiwara, T., T. Hoshino, T. Ooshima, and S. Hamada.** 2002. Differential and quantitative analyses of mRNA expression of glucosyltransferases from *Streptococcus mutans* MT8148. J. Dent. Res. **81:**109–113.
21. **Fukushima, K., T. Ikeda, and H. K. Kuramitsu.** 1992. Expression of *Streptococcus mutans gtf* genes in *Streptococcus milleri*. Infect. Immun. **60:**2815–2822.
22. **Gao, J., A. A. Gusa, J. R. Scott, and G. Churchward.** 2005. Binding of the global response regulator protein CovR to the sag promoter of *Streptococcus pyogenes* reveals a new mode of CovR-DNA interaction. J. Biol. Chem. **280:**38948–38956.
23. **Goodman, S. D., and Q. Gao.** 2000. Characterization of the *gtfB* and *gtfC* promoters from *Streptococcus mutans* GS-5. Plasmid **43:**85–98.
24. **Graham, M. R., L. M. Smoot, C. A. Migliaccio, K. Virtaneva, D. E. Sturdevant, S. F. Porcella, M. J. Federle, G. J. Adams, J. R. Scott, and J. M. Musser.** 2002. Virulence control in group A streptococcus by a two-component gene regulatory system: global expression profiling and in vivo infection modeling. Proc. Natl. Acad. Sci. USA **99:**13855–13860.
25. **Gusa, A. A., and J. R. Scott.** 2005. The CovR response regulator of group A streptococcus (GAS) acts directly to repress its own promoter. Mol. Microbiol. **56:**1195–1207.
26. **Hamada, S., and H. D. Slade.** 1980. Biology, immunology, and cariogenicity of *Streptococcus mutans*. Microbiol. Rev. **44:**331–384.
27. **Hoch, J. A., and K. I. Varughese.** 2001. Keeping signals straight in phosphorelay signal transduction. J. Bacteriol. **183:**4941–4949.
28. **Howell, A., S. Dubrac, K. K. Andersen, D. Noone, J. Fert, T. Msadek, and K. Devine.** 2003. Genes controlled by the essential YycG/YycF two-component system of *Bacillus subtilis* revealed through a novel hybrid regulator approach. Mol. Microbiol. **49:**1639–1655.
29. **Hudson, M. C, and R. Curtiss III.** 1990. Regulation of expression of *Streptococcus mutans* genes important to virulence. Infect. Immun. **58:**464–470.
30. **Hueck, C. J., W. Hillen, and M. H. Saier, Jr.** 1994. Analysis of a cis-active sequence mediating catabolite repression in gram-positive bacteria. Res. Microbiol. **145:**503–518.
31. **Husmann, L. K., D. L. Yung, S. K. Hollingshead, and J. R. Scott.** 1997. Role of putative virulence factors of *Streptococcus pyogenes* in mouse models of long-term throat colonization and pneumonia. Infect. Immun. **65:**1422–1430.
32. **Idone, V., S. Brendtro, R. Gillespie, S. Kocaj, E. Peterson, M. Rendi, W. Warren, S. Michalek, K. Krastel, D. Cvitkovitch, and G. Spatafora.** 2003. Effect of an orphan response regulator on *Streptococcus mutans* sucrose-dependent adherence and cariogenesis. Infect. Immun. **71:**4351–4360.
33. **Jiang, S. M., M. J. Cieslewicz, D. L. Kasper, and M. R. Wessels.** 2005. Regulation of virulence by a two-component system in group B streptococcus. J. Bacteriol. **187:**1105–1113.

34. **Kenney, L. J.** 2002. Structure/function relationships in OmpR and other winged-helix transcription factors. Curr. Opin. Microbiol. **5:**135–141.
35. **Ladds, J. C., K. Muchova, D. Blaskovic, R. J. Lewis, J. A. Brannigan, A. J. Wilkinson, and I. Barak.** 2003. The response regulator Spo0A from *Bacillus subtilis* is efficiently phosphorylated in Escherichia coli. FEMS Microbiol. Lett. **223:**153–157.
36. **Lamy, M. C., M. Zouine, J. Fert, M. Vergassola, E. Couve, E. Pellegrini, P. Glaser, F. Kunst, T. Msadek, P. Trieu-Cuot, and C. Poyart.** 2004. CovS/CovR of group B streptococcus: a two-component global regulatory system involved in virulence. Mol. Microbiol. **54:**1250–1268.
37. **Li, Y., and R. A. Burne.** 2001. Regulation of the *gtfBC* and *ftf* genes of *Streptococcus mutans* in biofilms in response to pH and carbohydrate. Microbiology **147:**2841–2848.
38. **Li, Y. H., P. C. Lau, N. Tang, G. Svensater, R. P. Ellen, and D. G. Cvitkovitch.** 2002. Novel two-component regulatory system involved in biofilm formation and acid resistance in *Streptococcus mutans*. J. Bacteriol. **184:**6333–6342.
39. **Loesche, W. J.** 1986. Role of *Streptococcus mutans* in human dental decay. Microbiol. Rev. **50:**353–380.
40. **Loo, C. Y., D. A. Corliss, and N. Ganeshkumar.** 2000. *Streptococcus gordonii* biofilm formation: identification of genes that code for biofilm phenotypes. J. Bacteriol. **182:**1374–1382.
41. **Ludwig, H., N. Rebhan, H. M. Blencke, M. Merzbacher, and J. Stulke.** 2002. Control of the glycolytic *gapA* operon by the catabolite control protein A in *Bacillus subtilis*: a novel mechanism of CcpA-mediated regulation. Mol. Microbiol. **45:**543–553.
42. **Ludwig, H., and J. Stulke.** 2001. The *Bacillus subtilis* catabolite control protein CcpA exerts all its regulatory functions by DNA-binding. FEMS Microbiol. Lett. **203:**125–129.
43. **Mattos-Graner, R. O., M. H. Napimoga, K. Fukushima, M. J. Duncan, and D. J. Smith.** 2004. Comparative analysis of Gtf isozyme production and diversity in isolates of *Streptococcus mutans* with different biofilm growth phenotypes. J. Clin. Microbiol. **42:**4586–4592.
44. **Miller, A. A., N. C. Engleberg, and V. J. DiRita.** 2001. Repression of virulence genes by phosphorylation-dependent oligomerization of CsrR at target promoters in *S. pyogenes*. Mol. Microbiol. **40:**976–990.
45. **Monchois, V., R. M. Willemot, and P. Monsan.** 1999. Glucansucrases: mechanism of action and structure-function relationships. FEMS Microbiol. Rev. **23:**131–151.
46. **Munro, C., S. M. Michalek, and F. L. Macrina.** 1991. Cariogenicity of *Streptococcus mutans* V403 glucosyltransferase and fructosyltransferase mutants constructed by allelic exchange. Infect. Immun. **59:**2316–2323.
47. **Nakano, Y. J., and H. K. Kuramitsu.** 1992. Mechanism of *Streptococcus mutans* glucosyltransferases: hybrid-enzyme analysis. J. Bacteriol. **174:**5639–5646.
48. **Ooshima, T., M. Matsumura, T. Hoshino, S. Kawabata, S. Sobue, and T. Fujiwara.** 2001. Contributions of three glycosyltransferases to sucrose-dependent adherence of *Streptococcus mutans*. J. Dent. Res. **80:**1672–1677.
49. **Que, Y. A., J. A. Haefliger, P. Francioli, and P. Moreillon.** 2000. Expression of *Staphylococcus aureus* clumping factor A in *Lactococcus lactis* subsp. *cremoris* using a new shuttle vector. Infect. Immun. **68:**3516–3522.
50. **Sato, Y., Y. Yamamoto, and H. Kizaki.** 1997. Cloning and sequence analysis of the *gbpC* gene encoding a novel glucan-binding protein of *Streptococcus mutans*. Infect. Immun. **65:**668–675.
51. **Sato, Y., Y. Yamamoto, and H. Kizaki.** 2000. Construction of region-specific partial duplication mutants (merodiploid mutants) to identify the regulatory gene for the glucan-binding protein C gene in vivo in *Streptococcus mutans*. FEMS Microbiol. Lett. **186:**187–191.
52. **Senadheera, M. D., B. Guggenheim, G. A. Spatafora, Y. C. Huang, J. Choi, D. C. Hung, J. S. Treglown, S. D. Goodman, R. P. Ellen, and D. G. Cvitkovitch.** 2005. A VicRK signal transduction system in *Streptococcus mutans* affects *gtfBCD*, *gbpB*, and *ftf* expression, biofilm formation, and genetic competence development. J. Bacteriol. **187:**4064–4076.
53. **Smorawinska, M., and H. K. Kuramitsu.** 1995. Primer extension analysis of *Streptococcus mutans* promoter structures. Oral Microbiol. Immunol. **10:**188–192.
54. **Stock, A. M., V. L. Robinson, and P. N. Goudreau.** 2000. Two-component signal transduction. Annu. Rev. Biochem. **69:**183–215.
55. **Ueda, S., and H. K. Kuramitsu.** 1988. Molecular basis for the spontaneous generation of colonization-defective mutants of *Streptococcus mutans*. Mol. Microbiol. **2:**135–140.
56. **Ueda, S., T. Shiroza, and H. K. Kuramitsu.** 1988. Sequence analysis of the gtfC gene from *Streptococcus mutans* GS-5. Gene **69:**101–109.
57. **Wagner, C., A. de Saizieu, H.-J. Schonfeld, M. Kamber, R. Lange, C. J. Thompson, and M. G. Page.** 2002. Genetic analysis and functional characterization of the *Streptococcus pneumoniae vic* operon. Infect. Immun. **70:**6121–6128.
58. **Warner, J. B., and J. S. Lolkema.** 2003. CcpA-dependent carbon catabolite repression in bacteria. Microbiol. Mol. Biol. Rev. **67:**475–490.
59. **Wexler, D. L., M. C. Hudson, and R. A. Burne.** 1993. *Streptococcus mutans* fructosyltransferase (*ftf*) and glucosyltransferase (*gtfBC*) operon fusion strains in continuous culture. Infect. Immun. **61:**1259–1267.
60. **Yamashita, Y., W. H. Bowen, R. A. Burne, and H. K. Kuramitsu.** 1993. Role of the *Streptococcus mutans gtf* genes in caries induction in the specific-pathogen-free rat model. Infect. Immun. **61:**3811–3817.
61. **Yoshida, A., T. Ansai, T. Takehara, and H. K. Kuramitsu.** 2005. LuxS-based signaling affects *Streptococcus mutans* biofilm formation. Appl. Environ. Microbiol. **71:**2372–2380.
62. **Yoshida, A., and H. K. Kuramitsu.** 2002. Multiple *Streptococcus mutans* genes are involved in biofilm formation. Appl. Environ. Microbiol. **68:**6283–6291.